

N 70 29980

**NASA TECHNICAL  
MEMORANDUM**

NASA TM X- 52808

NASA TM X- 52808

**BUOYANCY EFFECTS ON LIQUID NITROGEN  
FILM BOILING IN VERTICAL FLOW**

by S. S. Papell  
Lewis Research Center  
Cleveland, Ohio

**CASE FILE  
COPY**

**TECHNICAL PAPER No. G-2 for presentation at Cryogenic  
Engineering Conference sponsored by the National Academy  
of Sciences/National Research Council  
Boulder, Colorado, June 17-19, 1970**

**BUOYANCY EFFECTS ON LIQUID NITROGEN FILM BOILING IN VERTICAL FLOW**

by S. S. Papell

Lewis Research Center  
Cleveland, Ohio

**TECHNICAL PAPER No. G-2 for presentation at:**

**Cryogenic Engineering Conference**

sponsored by the National Academy of Science/National Research Council  
Boulder, Colorado, June 17-19, 1970

**NATIONAL AERONAUTICS AND SPACE ADMINISTRATION**

BUOYANCY EFFECTS ON LIQUID NITROGEN  
FILM BOILING IN VERTICAL FLOW

by S. S. Papell

Lewis Research Center  
National Aeronautics and Space Administration  
Cleveland, Ohio

ABSTRACT

Liquid nitrogen film boiling data were obtained for upward and downward flow through a resistance heated test section with 0.505-inch inside diameter and a 12-inch heated length. Test conditions include a pressure range from 35 to 200 psia at inlet velocities from 1.7 to 7.5 ft/sec over a range of heat fluxes from 0.007 to 0.052 Btu/sec in<sup>2</sup>. Inlet subcooling varied from saturation at 35 psia to 45° R at 200 psia.

Subject to the test conditions examined, it was found that under comparative heat fluxes and flow rates the wall temperatures for downflow could be up to 750° R higher than for upflow. This temperature difference represents a heat-transfer coefficient for the upflow case over 8 times greater than for the downflow case. A maximum inlet velocity of about 7.5 ft/sec and a system pressure of about 100 psia were found to define the limits below which buoyancy can influence the forced convection film boiling system used in this study. The results were discussed in terms of differences in vapor film thickness and local void distribution as influenced by buoyancy, velocity, pressure, and subcooling.

NOMENCLATURE

$C_p$	specific heat
$D$	diameter
$g$	gravity acceleration
$h$	heat transfer coefficient
$k$	thermal conductivity

L	length of test section
p	pressure
Q	heat flow
q	heat flux
T	temperature
V	velocity
x	local position measured from inlet
$\mu$	absolute viscosity
$\rho$	density
$\lambda$	heat of vaporization
$\lambda'$	from Eq. (5)

#### Subscripts

avg	average
b	bulk
D	downflow
F	fluid
i	fluid side surface
l	local
m	metal
o	outside surface
s	saturated
U	upflow

### INTRODUCTION

Film boiling occurs when a continuous vapor film exists between the heat transfer surface and the liquid. The evaporation of liquid is essentially on the liquid-vapor interface with heat transfer across the

film primarily by conduction. This mode of heat transfer has been analyzed for both the pool (nonflow) and forced flow system. In these analyses, both buoyancy and viscous forces are known to influence the thickness and stability of the vapor film which are recognized as controlling parameters in this heat transport mechanism.

For the pool film boiling case the buoyancy force is the prime vapor removal mechanism and its influence on heat transfer is documented in various publications, examples of which are found in references 1 and 2. Both drop towers and centrifuge devices were used to subject pool systems to other than Earth gravity. Increased gravity forces resulted in thinner vapor films and higher heat transfer rates while at reduced gravity lower heat transfer rates were caused by a thickening of the vapor film.

For the forced convection film boiling case both buoyancy and viscous forces caused by wall and interfacial shear are significant with viscous forces becoming predominant at higher fluid velocities. This phenomena is neatly illustrated by Bromley in reference 3 which presents an analysis that results in two correlating equations for different velocity regimes. The low velocity correlation which was originally for free convection contained a buoyancy term without a velocity term while the opposite was true for the higher velocity correlation. The analysis and data from reference 3 hold for a flow system characterized by cross flow around a heat transfer cylinder submerged in a moving fluid. The free convection correlation was extended by Hsu references 4 and 5 to describe film boiling from a long vertical plate.

A visual study was made by Simoneau (ref. 6) to demonstrate the influence of buoyancy on a liquid nitrogen boiling heat transfer system characterized by internal vertical flow parallel to a heat transfer strip. Film boiling high speed photographs taken under comparative test conditions for low velocity upflow and downflow showed a much larger accumulation of vapor for the downflow case than for the upflow case.

The present study was aimed at examining the extent that this change in void distribution could effect the heat transfer involved. The apparatus consisted of an instrumented test section as part of a liquid nitrogen flow system capable of being oriented so that fluid flow could be either in the direction of or opposed to the Earth gravity vector. The resulting change in buoyancy is defined as plus or minus one "g" with respect to the flow direction. This same technique was used by the author reference 7 to determine the effect of buoyancy on the critical heat flux in vertical flow. The present data were obtained in both flow directions through a resistance heated test section with a 0.505-inch diameter and a 12-inch heated length. Test conditions included a pressure range from 35 to 200 psia at inlet velocity variations from 1.7 to 7.5 ft/sec over a range of heat fluxes from 0.007 to 0.052 Btu/sec in.<sup>2</sup>. The inlet subcooling varied from zero degrees at 35 psia to 45° R at 200 psia.

## APPARATUS

### Flow System

The experimental apparatus used to obtain the film boiling data is shown in figure 1. The system was composed of three integral units that include a helium gas high pressure storage sphere mounted in an insulated cylindrical tank, a 40-gallon liquid nitrogen supply Dewar, and a cylindrical vacuum tank containing the test section.

The helium gas used to pressurize the Dewar was precooled by a liquid nitrogen both to minimize heat transfer between the gas and the working fluid. The nitrogen was forced to flow through the system and discharge to the atmosphere. Upstream and downstream of the test section were mixing chambers designed to eliminate temperature stratification in the bulk fluid. Flow rates and system pressures were controlled by throttling valves located at the top of the Dewar and downstream of the test section tank. The entire flow system between the two control valves was vacuum-jacketed to minimize external heat leaks.

The Dewar and the test section tank were installed within an angle-iron cage mounted on trunnion-type supports to allow for rotation. The helium supply sphere in the liquid nitrogen bath was coupled to the Dewar by means of a flexible high pressure hose. This arrangement made it possible to turn the test section over without changing the flow system.

### Test Sections

Figure 2(a) schematically describes the physical dimensions and instrumentation locations of the test section used in this study. It was made of inconel X tubing having an inside diameter of 0.505-inch; a 0.010-inch wall thickness and a 12-inch heated length.

A uniform heat flux was generated by a 10,000-watt, 400 hertz alternator using the test section as a resistance heater. The power was controlled by a variable transformer that delivered a maximum of 16 volts and 600 amps to the test section.

### Instrumentation

The vertical orientation of the test section mounted within the vacuum tank is shown schematically in figure 2(b). The outer surface temperatures were measured by 12 copper-constantan thermocouples made of 28-gage wire that were silver soldered in 2 rows 180° apart on the circumference of the tube. Five voltage taps made of 28-gage copper wire were installed along the tube to verify the linearity of the voltage drop. Fluid bulk temperature measurements were made with platinum resistance thermometers located in the mixing chambers. System pressures measured in the mixing chambers showed an average pressure drop across the test section of less than 1 psia.

The power to heat the test section was measured in terms of volts and amps. The output signals were converted to low-voltage direct current for recording purposes. These millivolt signals, along with the outputs of the pressure transducers, resistance thermometers

and thermocouples were fed to a central data acquisition system and recorded on magnetic tape. The signals were isolated and split before going to the voltage digitizer and sent to a multichannel oscillograph for visual monitoring of the tests.

### Experimental Procedure

The cage containing the Dewar and the test section tank was initially mounted on the trunnion supports with the test section oriented to permit upward fluid flow. Calibrations were made and repeated prior to each run using standard instruments to assure measurement accuracy. The cool down period was initiated by filling the liquid nitrogen bath tank within which the helium gas supply sphere was submerged. The 40-gallon Dewar was then filled while venting through the test section. In this manner, the residual heat stored in both the Dewar and the flow system was removed. The cool down and filling period was followed by data acquisition through the following systematic-running procedure.

The controlled test variables were system pressure, fluid flow rate, and heat flux. With the pressure and flow rate set at some predetermined value a data run was initiated by applying a step input of power of sufficient magnitude to induce film boiling over the entire test section length. Steady state conditions were verified by the oscillograph traces before the data were recorded. The power input was reduced by small increments and the data recorded until the vapor film started to collapse as indicated by the start of transition to nucleate boiling. This condition specified the termination of each run which was made over a range of flow rates at different system pressures. A guard heater on the inlet side electrode made it possible to extend the range of heat fluxes to much lower values by delaying the transition to nucleate boiling.

The cage containing the Dewar and test section tank was then rotated on the trunnion supports so that fluid flow was in a downward direction. Removal of the dip tube from the Dewar was required to per-



mit fluid to flow with the apparatus in this orientation. The same running procedure was used to repeat the test conditions under which the upflow data were obtained. Since the only difference in test conditions downstream of the inlet control valve for the two sets of data was the direction of fluid flow any difference in the data had to reflect the change in buoyancy force.

The data obtained are presented graphically and cover a range of pressures from 35 to 200 psia at inlet velocities from 1.7 to 7.5 ft/sec over a range of heat fluxes from 0.007 to 0.052 Btu/sec in.<sup>2</sup>. The inlet subcooling varied from zero at 35 psia to 45° at 200 psia.

## EXPERIMENTAL DATA

### Typical Basic Data

Figure 3 is an example of a data run showing the change in fluid side wall temperature profile as a function of heat flux for the case of upward flow. The test conditions include a system pressure of 35 psia and a flow rate of 0.22 lbs/sec which represents an inlet velocity of 3.5 ft/sec. The liquid nitrogen inlet bulk temperature for all the 35 psia data runs was at saturation conditions. The fluid side wall temperatures were calculated from outside wall temperature measurements by an equation from reference 8 that assumes uniform internal power generation:

$$T_i = T_o - k \frac{Q}{k_m} \quad (1)$$

where

$$k = \frac{r_o^2 \ln \frac{r_o}{r_i} - \left( \frac{r_o^2 - r_i^2}{2} \right)}{2\pi L (r_o^2 - r_i^2)} \quad (2)$$

The apparent change in temperature profiles in figure 3 over the range of heat fluxes from 0.007 to 0.052 Btu/sec in.<sup>2</sup> will not be dis-

cussed herein since this paper is primarily concerned with the effects of changes in buoyancy that will be examined by data comparisons under the same test conditions. Lavery and Rohsenow (ref. 9) present similar saturated type upflow data along with a discussion of their data trends. A limited data correlation of the 35 psia upflow data was made using an equation presented by Hsu reference 4. The results are described in the appendix.

#### Upflow Data

The present data were analyzed at a position along the tube that had a flat temperature profile. This was done to take advantage of temperature averaging because of data scatter at the higher heat fluxes. The position chosen was 7 inches from the inlet at an  $x/D$  of 14 using average values from the measuring stations equally spaced on either side. Figure 3 will show that the temperature profiles are rather flat at this position so that their values actually represent most of the data downstream of the first 4 inches of the test section.

Figure 4 presents the upflow 35 psia data showing the change in fluid side wall temperature at  $x/D = 14$  as a function of heat flux over a range of flow rates from 0.15 to 0.49 lbs/sec. The data represents an inlet velocity range from 2.2 to 7.5 ft/sec over which the wall temperature are not appreciably influenced by this change in velocity. The solid line drawn through these data points is quite representative and will be compared to the results obtained from the downflow tests.

#### Downflow Data

The downflow 35 psia data is presented on figure 5 over a range of flow rates from 0.10 to 0.48 lb/sec. This represents an inlet velocity range from 1.7 to 7.5 ft/sec which is similar to the upflow data on figure 4. In contrast to upflow as represented by the dashed line on this plot, the downflow data appears to be considerably influenced by

changes in fluid velocity. The solid lines connecting the data points form a family of curves that are unique for each flow rate. Largest divergence of this data from the upflow curve is the lower velocity data at an inlet velocity of 1.7 ft/sec. As the velocity is increased the average slope of the lines increase until at a velocity of 7.5 ft/sec the upflow and downflow curves coincide.

An order of magnitude examination of the difference in wall temperatures on figure 5 will show that at a heat flux of about 0.01 Btu/sec in.<sup>2</sup> the wall temperature can range in value from 350° to 1000° R. These differences in temperature depend on fluid velocity and/or flow direction.

## EFFECT OF BUOYANCY ON HEAT TRANSFER

### Flow Model

Since the only change in test conditions for the upflow and downflow case was the direction of flow with respect to the buoyancy force the difference in the data must be attributed to the manner in which this body force influences the flow system. The higher wall temperatures for the downflow case can be due to radical changes in local void distribution that increases as the flow rate is reduced. The vapor is acted on by the buoyancy force and tends to accumulate in the system. This phenomena of downward flow vapor accumulation has been demonstrated by means of the photographic study of reference 6 described in the INTRODUCTION.

A hydrodynamic heat transfer model of film boiling in a tube at a position of  $x/D = 14$  from the inlet can be described as consisting of two distinct parts. This includes a vapor annulus on the wall and some type of vapor-liquid inner core flow. Under certain test conditions both parts of the this flow system can be influenced by buoyancy. The accumulation of vapor in the core flow may effect the bulk temperature to some extent but it is suggested that the main reason for the higher wall temperatures in downward flow is a thickening of the vapor film on the wall of the test section.

The influence of buoyancy on the flow system used for this study diminishes as the flow rate is increased and finally vanishes at an inlet velocity of 7.5 ft/sec.

#### Magnitude of Buoyancy Effect

The magnitude of the influence of buoyancy on film boiling is illustrated on figure 6 in terms of a heat-transfer coefficient ratio as a function of inlet velocity. The heat transfer coefficient is defined as heat transfer from the fluid side wall temperature to the bulk fluid calculated at saturation conditions.

$$q = h(T_i - T_s) \quad (3)$$

If subscripts designating upflow and downflow are included a ratio of these equations will result in the following relation:

$$\frac{h_U}{h_D} = \frac{q_U (T_{i,D} - T_s)}{q_D (T_{i,U} - T_s)} \quad (4)$$

An examination of equation (4) will show that data compared at a constant wall temperature ( $T_s$ ) will satisfy the relation that the heat flux ratio is equal to the heat-transfer coefficient ratio. Figure 6 illustrates this fact by satisfying the equation at a constant wall temperature of 800° R with data obtained from figure 5. An examination of figure 6 at an inlet velocity of 1.7 ft/sec will show that the heat transfer coefficient for the upflow case is over 8 times greater than for the downflow case. The influence of buoyancy decreases rapidly at an inlet velocity of 2.5 ft/sec and vanished at 7.5 ft/sec. For this particular set of data we can establish a Froude No. Criterion of  $V^2/Dg = 42.3$  below which buoyancy can influence the heat transfer involved.

Treating the figure 5 data at different wall temperatures in the same manner will show that the magnitude of the buoyancy effect on heat transfer is a function of both flow rate and heat flux for a given wall temperature or ( $\Delta T$ ).

### Influence of Pressure and Inlet Subcooling

The discussion of the influence of buoyancy on forced convection film boiling up to now only applies to saturated inlet data obtained at a system pressure of 35 psia. Although the effect of pressure is not within the scope of this paper a limited amount of higher pressure data is presented in figure 7 to illustrate a general trend in the data.

The heat flux or heat transfer coefficient ratio is plotted as a function of pressure for data limited to a wall temperature of  $800^{\circ}$  R at an inlet velocity of 1.7 ft/sec. These high temperature and low velocity test conditions were chosen as being representative of data that should be considerably influenced by buoyancy. From the plot (fig. 7) it appears that an increase of pressure decreases the effect of buoyancy on this flow system. The decrease is quite rapid up to a pressure of about 75 psia and is eliminated completely at 100 psia which represents a critical pressure ratio  $p/p_c$  equal to 0.203.

Unfortunately, the effect of inlet subcooling cannot be isolated from the effect of pressure because the change in inlet subcooling varied from saturation at 35 psia to a  $(\Delta T)_s$  of  $45^{\circ}$  R at 200 psia. It should be noted, though, that at an inlet velocity of 1.7 ft/sec the enthalpy rise was sufficient to saturate the bulk fluid at the position chosen ( $x/D = 14$ ) for all the data. The main difference in flow conditions that was not controlled is the local void distribution. Rapid elimination of the effect of buoyancy at increased pressures as seen on figure 8 may be primarily do to these differences in inlet subcooling.

### SUMMARY OF RESULTS

An experimental study was made to examine the effect of buoyancy on a liquid nitrogen film boiling system in vertical flow. A change in buoyancy was effected by reversing the flow direction with respect to the Earth gravity vector. Film boiling data were obtained for upward and downward flow through a resistance heated test section with a 0.505-inch inside diameter and a 12-inch heated length. Test condi-

tions include a pressure range from 35 to 200 psia at inlet velocities from 1.7 to 7.5 ft/sec over a range of heat fluxes from 0.007 to 0.052 Btu/sec in.<sup>2</sup>. Inlet subcooling varied from zero degrees at 35 psia to 45° R at 200 psia. The following results obtained by comparison of the up and downflow data are subject to the test conditions and flow geometry used in this study:

(1) The downflow data were significantly influenced by changes in flow rates while the upflow data were not.

(2) Under comparative heat fluxes and flow rates the wall temperatures for downflow were up to 750° R higher than for upflow with the temperature differences decreasing with increased flow rates.

(3) Under comparative heat fluxes and flow rates the heat-transfer coefficients can be over 8 times greater for the upflow case than for the downflow case.

(4) For the 35 psia data at saturation inlet conditions a maximum inlet velocity of about 7.5 ft/sec (Froude No.  $V^2/Dg = 42.3$ ) was found to define the limit below which buoyancy can influence forced convection film boiling. It is suggested that this maximum should be a function of diameter, pressure, inlet subcooling and location on the tube.

(5) A maximum pressure of about 100 psia at an inlet subcooling of 45° R was found to define the limit below which buoyancy can influence forced convection film boiling.

(6) The phenomena described above were discussed in terms of differences in vapor film thickness and local void distribution as influenced by buoyancy, velocity, pressure and subcooling.

## APPENDIX

Bromley, in reference 3 showed that the influence of forced convection is negligible at low velocities for film boiling off a horizontal rod in cross-flow. Thus, for the range of conditions examined he concluded that his free convection film boiling equation could apply provided the velocity relation  $(U/\sqrt{gD})$  was less than 2. Since Bromley's analysis has been extended by Hsu references 4 and 5 to describe film boiling off a long vertical plate it was used in attempting to correlate the present data. The equation follows:

$$h_l = 0.603 \left[ \frac{k_f^3 (\rho_L - \rho_v) \rho_v g \lambda'}{x(\Delta T)u} \right]^{1/4} \quad (5)$$

where

$$\lambda' = \lambda \left[ 1 + \frac{0.4(\Delta T)C_p}{\lambda} \right]^2$$

The heat transfer coefficient is a local value at the distance  $l$  from the start of the heated length. The equation coefficient of 0.603 suggested by Hsu is dependent on the assumed boundary conditions at the liquid-vapor interface.

It should be noted that the analysis used in the derivation of equation (5) required the existence of laminar vapor flow. Therefore to satisfy this restriction the present data that can be applied were taken from the first wall temperature measuring station located 0.75 inches from the inlet. A sampling of the 35 psia, upflow, liquid nitrogen, saturated inlet data is shown in figure 8. The local measured heat transfer coefficient divided by the functional grouping of parameters from equation (5) is plotted against the velocity relation  $U_l/\sqrt{gx}$ . Local velocity is based on an equilibrium type of calculation using local density obtained from local quality. A definite data trend with

velocity is shown which should be expected. The dashed line represents the equation constant of 0.603 extended to intersect the correlated data line at  $U_l/\sqrt{gx} \approx 2$  which is similar to Bromley's reference 3 results. But, without a knowledge of the relation between the geometry parameters in both test facilities these results can only be considered coincidental.



## REFERENCES

1. Heath, C. A.; Costello, C. P.: The Effect of the Orientation and Magnitude of Gravity Fields on Film Boiling from a Flat Plate. U. of Wash., College of Engineering, May 1964.
2. Pomerantz, M. L.: Film Boiling on a Horizontal Tube in Increased Gravity Fields. ASME Paper No. 63-HT-17, 1963.
3. Bromley, L. A.; LeRoy, N. R. and Robbers, J. A.: Heat Transfer in Forced Convection Film Boiling. Industrial and Engineering Chem., vol. 45, no. 12, 1953, pp. 2639-2646.
4. Hsu, Y. Y.: PhD Thesis, University of Illinois, URBANA (1958).
5. Hsu, Y. Y.; and Westwater, J. W.: Approximate Theory For Film Boiling on Vertical Surfaces. Chemical Eng. Prog. Symposium Series, Vol. 56, no. 30, 1960.
6. Simoneau, R. J.; Simon, F. F.: A Visual Study of Velocity and Buoyancy Effects on Boiling Nitrogen. NASA TN D-3354, Sept. 1966.
7. Papell, S. S.; Simoneau, R. J.; and Brown, D. D.: Buoyancy Effects on Critical Heat Flux of Forced Convective Boiling in Vertical Flow. NASA TN D-3672, 1966.
8. McAdams, W. H.: Heat Transmission. 3rd Ed., McGraw-Hill Book Co., p. 19.
9. Laverty, W. F.; and Rohsenow, W. M.: Film Boiling of Saturated Liquid Flowing Upward Through a Heated Tube: High Vapor Quality Range. TR No. 9857-32, Dept. of Mech. Eng., MIT, Sept. 1964.

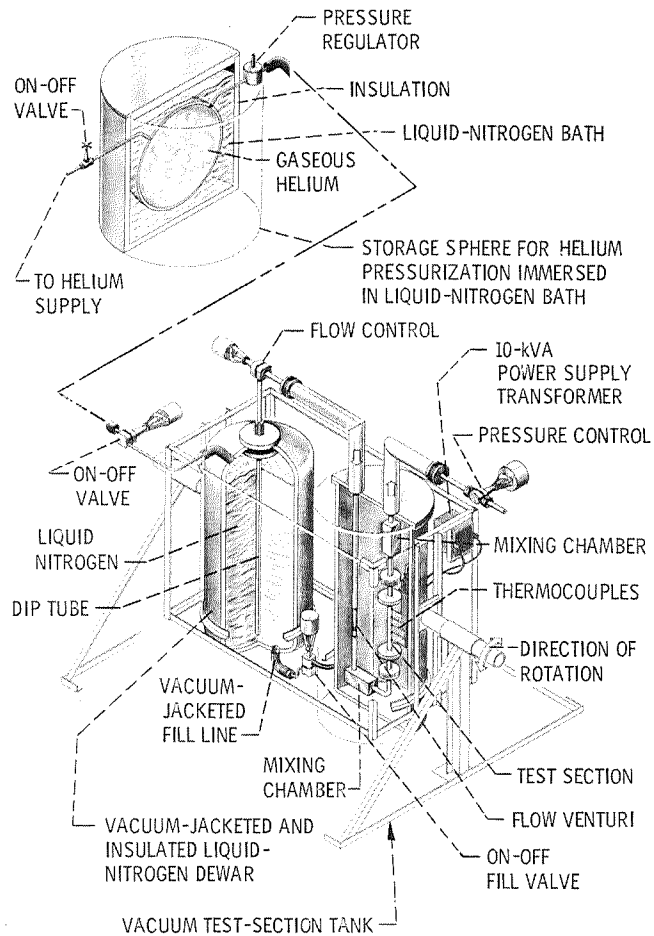


Figure 1. - Liquid-nitrogen heat-transfer apparatus.

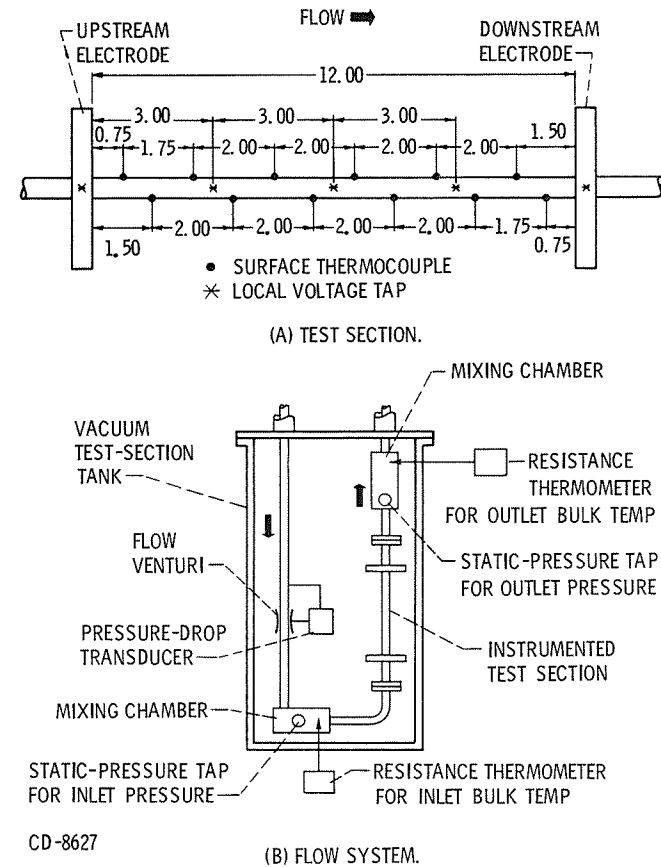


Figure 2. - Instrumentation. (All dimensions are in inches.)

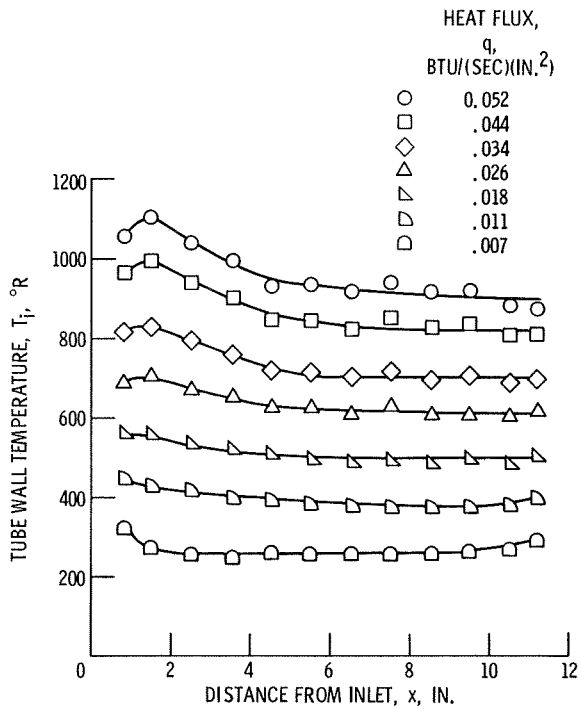


Figure 3. - Basic film boiling data - upflow - liquid nitrogen; 35 psia; flow rate, 0.22 lb/sec, inlet bulk temperature, 153° R.

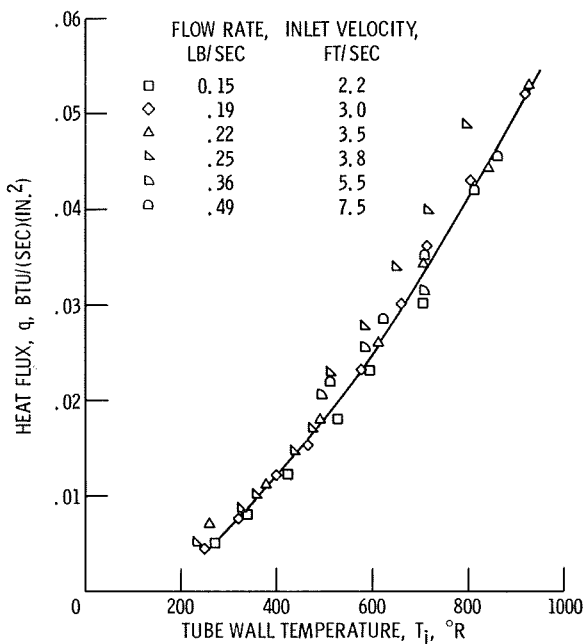


Figure 4. - Upflow film boiling data. Liquid nitrogen; 35 psia;  $x/D$ , 14; inlet bulk temperature, 153° R.

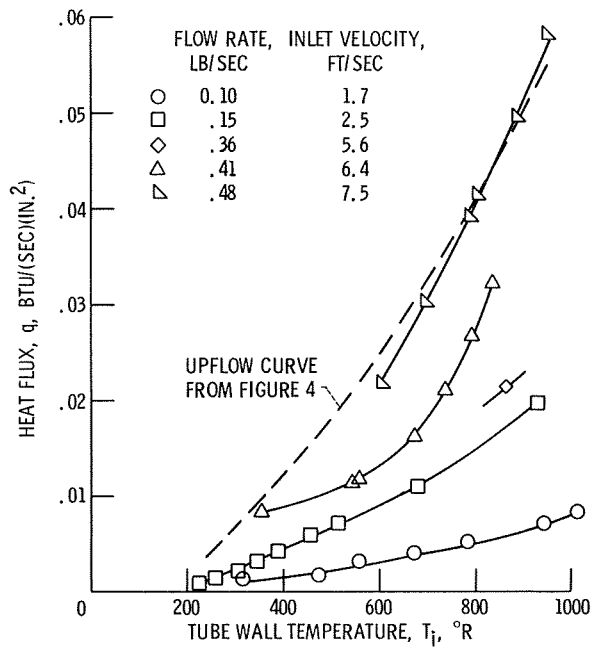


Figure 5. - Downflow film boiling data. Liquid nitrogen; 35 psia;  $x/D$ , 14; inlet bulk temperature, 153° R.

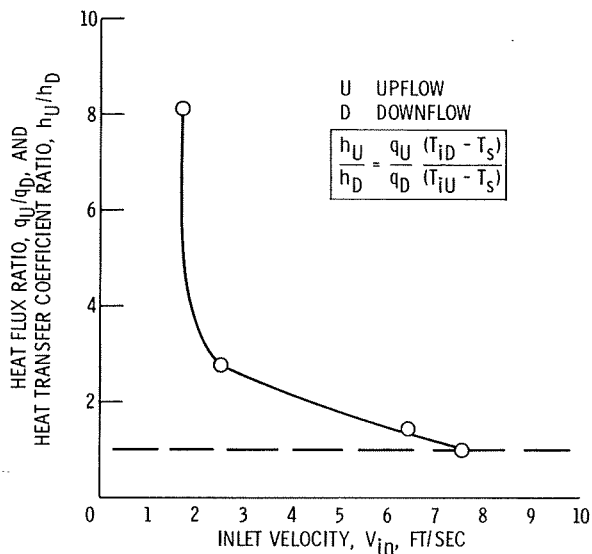


Figure 6. - Effect of velocity on buoyancy influence on film boiling. Upflow and downflow data from figure 5.  $T_i$ , 800° R; liquid nitrogen; 35 psia;  $x/D$ , 14.

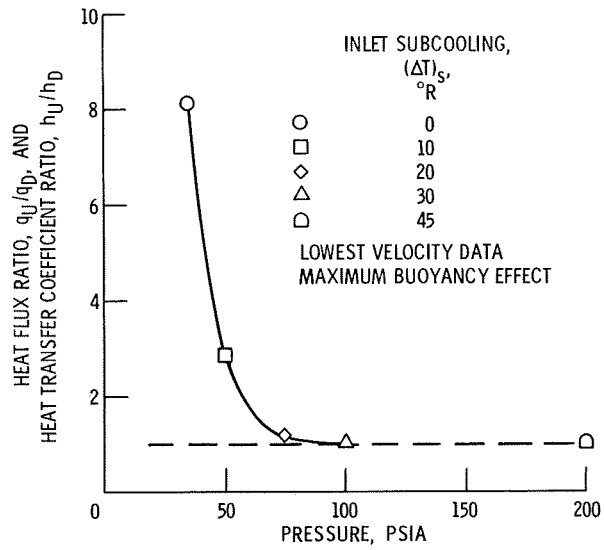


Figure 7. - Pressure and subcooling effect of buoyancy influence on film boiling.  $T_i$ , 800° R;  $V_{in}$ , 1.7 ft/sec;  $x/D$ , 14.

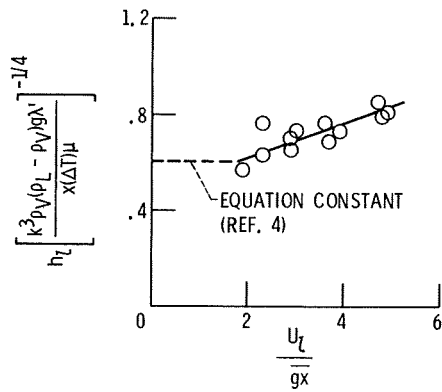


Figure 8. - Upflow film boiling data correlation. Liquid nitrogen; 35 psia;  $x = 0.75$  inch;  $x/D$ , 1.5; saturated inlet bulk conditions.